Downloaded from http://polymerphysics.net

Macromolecules
ARTICLE

Macromolecules **2011**, *44*, 1149–1155 **1149**
DOI: 10.1021/ma102795w

Dynamic Heterogeneity and Density Scaling in 1,4-Polyisoprene

D. Fragiadakis,[†] R. Casalini,[†] R. B. Bogoslovov,[†,‡] C. G. Robertson,[§] and C. M. Roland*[,†]

[†]*Naval Research Laboratory, Code 6120, Washington, D.C. 20375-5342, United States,* [‡]*Enterprise Sciences, Inc., College Park, Maryland 20740, United States, and* [§]*Bridgestone Americas, Center for Research and Technology, 1200 Firestone Parkway, Akron, Ohio 44317-0001, United States*

Received December 9, 2010; Revised Manuscript Received January 13, 2011

ABSTRACT: Dielectric relaxation times were measured for 1,4-polyisoprenes (PI) of different molecular weight. From the data, the number of dynamically correlated segments, N_c, was calculated using an approximation to the dynamic susceptibility. N_c increases with approach to the glass transition in the usual fashion and also increases with increasing molecular weight of the PI. The latter effect is ascribed to the loss of the configurational mobility conferred by the chain ends. The correlation volume was also estimated from calorimetry and, because PI has a dielectrically active normal mode, from the intersection of the extrapolated segmental and normal mode relaxation times. The three methods yield consistent results, although the last has large uncertainty due to the ambiguous connection between dynamic correlation lengths and volumes. Using the equation of state for the polymers, the dependence of the relaxation times on the scaling variable TV^{γ}, where V is specific volume and γ is a material constant, was calculated. For the lowest molecular weight PI, there is a small difference in γ for the segmental and chain modes. The scaling exponent is also marginally smaller for the lower molecular weight sample, suggesting, in contrast with the behavior of other polymers, that in PI the volume dependence becomes weaker with decreasing molecular weight.

Introduction

In the dielectric loss spectrum of polymers having a dipole moment parallel to the chain ("type-A polymers"[1]), there is a relaxation peak corresponding to motion of the chain end-to-end vector.[2,3] The behavior of this loss peak reflects the chain dynamics, enabling dielectric spectroscopy to be used to investigate rheological properties. One issue is the weaker effect of temperature and pressure on the frequency of this peak, in comparison with their effect on the local segmental dynamics;[4−7] this remains an incompletely understood phenomenon in polymer viscoelasticity. Unfortunately, there is only a handful of polymers with dielectrically active normal modes; these include polylactides,[8] polyoxybutylene,[9,10] polypropylene glycol (PPG),[6,11−13] poly(*n*-hexyl isocyanate),[14] polystyrene oxide,[15] and 1,4-polyisoprene (PI).[3,5,11,16−21] In this Article, we report measurements on PI of differing molecular weights.

Two properties of glass-forming liquids and polymers are of particular interest herein. The first concerns the heterogeneity of the dynamics. Spatial variations lead to a dynamic correlation volume, defined from the maximum in the four-point dynamic susceptibility, $\chi_4(t)$. $\chi_4(t)$ quantifies the correlation in space and time of the molecular motions, and although it can be expressed as the variance of the self-intermediate scattering function,[22] it cannot be determined from conventional dielectric relaxation measurements. However, Berthier and coworkers[23−25] proposed an approximation, $\chi_T(t)$, for the number of dynamically correlated molecules or polymer segments

$$N_c \geq \frac{N_A}{m}\frac{k_B}{\Delta c_p}T^2 \max\left(\frac{\partial \varepsilon}{\partial T}\right)^2 \quad (1)$$

where m is the repeat unit molecular weight, N_A is Avogadro's number, Δc_p is the isobaric heat capacity change at T_g, and k_B is the Boltzmann constant. In eq 1, ε represents the dielectric relaxation function, but other experimentally accessible linear susceptibilities can be utilized. The derivation of $\chi_T(t)$ assumes that the dynamics are driven mainly by temperature fluctuations, neglecting the effect of density. This neglect means that the N_c calculated from $\chi_T(t)$ is a lower bound on the actual N_c. The magnitude of this difference between the actual and approximate N_c is chemical-species-dependent[26] and grows as τ_α decreases. We evaluate N_c from χ_T for the different molecular weight PI to determine whether the concentration of chain ends, associated with excess configurational entropy and mobility, affects the correlation of the dynamics. We also assess dynamic heterogeneity at T_g from calorimetry using the method of Donth[27] and by a procedure proposed by Schönhals and Schlosser[28] based on convergence at low temperature of the normal mode, τ_N, and segmental, τ_α, relaxation times. The merging of the respective τ occurs when the length scale of the dynamic correlations for the α-relaxation matches the spatial extent of the chain molecules, reflected in the dielectric normal mode. These dynamic correlations are primarily intermolecular and distinct from the intrachain correlations accompanying the conformational transitions of even isolated chains.[29]

The second property of interest herein is the superposition of segmental relaxation times for various state points when plotted according to[30,31]

$$\tau_\alpha = f(TV^{\gamma}) \quad (2)$$

where f is a function, V is the specific volume, and γ is a material constant. Previously, we showed that eq 2 applies to normal mode relaxation times using the same value of the exponent γ as that for the segmental relaxation times.[10,11] We scrutinize this behavior for different molecular weights, with measurements extending over a broader dynamic range than the prior experiments on PI.[11]

*To whom correspondence should be addressed.

© 2011 American Chemical Society

Published on Web 02/04/2011

Report Documentation Page

Form Approved
OMB No. 0704-0188

Public reporting burden for the collection of information is estimated to average 1 hour per response, including the time for reviewing instructions, searching existing data sources, gathering and maintaining the data needed, and completing and reviewing the collection of information. Send comments regarding this burden estimate or any other aspect of this collection of information, including suggestions for reducing this burden, to Washington Headquarters Services, Directorate for Information Operations and Reports, 1215 Jefferson Davis Highway, Suite 1204, Arlington VA 22202-4302. Respondents should be aware that notwithstanding any other provision of law, no person shall be subject to a penalty for failing to comply with a collection of information if it does not display a currently valid OMB control number.

1. REPORT DATE	2. REPORT TYPE	3. DATES COVERED
2011		**00-00-2011 to 00-00-2011**

4. TITLE AND SUBTITLE	5a. CONTRACT NUMBER
Dynamic Heterogeneity And Density Scaling In 1,4-Polyisoprene	5b. GRANT NUMBER
	5c. PROGRAM ELEMENT NUMBER
6. AUTHOR(S)	5d. PROJECT NUMBER
	5e. TASK NUMBER
	5f. WORK UNIT NUMBER
7. PERFORMING ORGANIZATION NAME(S) AND ADDRESS(ES)	8. PERFORMING ORGANIZATION REPORT NUMBER
Naval Research Laboratory, Code 6120,Washington,DC,20375	
9. SPONSORING/MONITORING AGENCY NAME(S) AND ADDRESS(ES)	10. SPONSOR/MONITOR'S ACRONYM(S)
	11. SPONSOR/MONITOR'S REPORT NUMBER(S)

12. DISTRIBUTION/AVAILABILITY STATEMENT

Approved for public release; distribution unlimited

13. SUPPLEMENTARY NOTES

Macromolecules 2011, 44, 1149-1155

14. ABSTRACT

Dielectric relaxation times were measured for 1,4-polyisoprenes (PI) of different molecular weight. From the data, the number of dynamically correlated segments, Nc, was calculated using an approximation to the dynamic susceptibility. Nc increases with approach to the glass transition in the usual fashion and also increases with increasing molecular weight of the PI. The latter effect is ascribed to the loss of the configurational mobility conferred by the chain ends. The correlation volume was also estimated from calorimetry and, because PI has a dielectrically active normal mode, from the intersection of the extrapolated segmental and normal mode relaxation times. The three methods yield consistent results, although the last has large uncertainty due to the ambiguous connection between dynamic correlation lengths and volumes. Using the equation of state for the polymers, the dependence of the relaxation times on the scaling variable TVγ,where V is specific volume and γ is a material constant, was calculated. For the lowest molecular weight PI,there is a small difference in γ for the segmental and chain modes. The scaling exponent is also marginally smaller for the lower molecular weight sample, suggesting, in contrast with the behavior of other polymers,that in PI the volume dependence becomes weaker with decreasing molecular weight.

15. SUBJECT TERMS

16. SECURITY CLASSIFICATION OF:			17. LIMITATION OF ABSTRACT	18. NUMBER OF PAGES	19a. NAME OF RESPONSIBLE PERSON
a. REPORT	b. ABSTRACT	c. THIS PAGE			
unclassified	**unclassified**	**unclassified**	**Same as Report (SAR)**	**8**	

Table 1. Glass-Transition Temperatures and Number of Correlated Repeat Units for 1,4-Polyisoprene

	degree of polymerization	T_g (DSC) [K][a]	T (τ_α = 1 s) [K][a]	N_c (τ_α = 1 s)
PI-1	18	191.5	193.9	130
PI-10	145	206.2	210.9	155
PI-20	312	207.3	212.6	180

[a] P = 0.1 MPa.

Experimental Section

The polyisoprene samples were: PI-1 (M_w = 1.20 kg/mol, M_n = 1.10 kg/mol) from Polymer Source, Canada, PI-10 (M_w = 9.91 kg/mol, M_n = 9.73 kg/mol), and PI-20 (M_w = 21.2 kg/mol, M_n = 20.7 kg/mol) from Polymers Standards Service. The degrees of polymerization (DP) are listed in Table 1. Modulated differential scanning calorimetry (MDSC) was performed using a TA Instruments model Q2000 calorimeter. Samples (ca. 7 mg) were cooled to the glassy state at 5 K/min and then measured using the same heating rate with a superimposed temperature modulation amplitude of 0.5 K with a 40 s period. A sapphire control sample was used to calibrate the heat capacity. Pressure−volume−temperature (PVT) measurements employed a Gnomix instrument.[32] Temperature was decreased at 0.5 K/min at various fixed pressures up to 200 MPa. The ambient density was measured by the buoyancy method. Dielectric spectroscopy measurements were carried out with the samples (after 24 h of drying in vacuo) between circular electrodes (15 mm diameter) with a 0.2 mm PTFE spacer to maintain a constant thickness. Spectra were obtained using a Novocontrol Alpha analyzer (10^{-2} to 10^6 Hz) and an IMASS time domain dielectric analyzer (10^{-4} to 10^3 Hz). For ambient pressure measurements, a closed-cycle helium cryostat was used to control temperature to within 0.02 K. For elevated pressure measurements (on PI-1 and PI-20 only), the sample capacitor assembly was contained in a Manganin cell (Harwood Engineering) with pressure applied using a hydraulic pump (Enerpac) in combination with a pressure intensifier (Harwood Engineering). Pressures were measured with a Sensotec tensometric transducer (150 kPa resolution) and a Heise pressure gauge (70 kPa accuracy). A Tenney Jr. chamber was used for temperature control (±0.1 K at the sample).

Results and Discussion

Representative dielectric loss spectra are shown in Figure 1 for PI-1, the lowest M_w sample, which thus has greatest overlap of the segmental and normal mode relaxations. To determine the respective τ, it is necessary to deconvolute the peaks by fitting the spectra. For the segmental peak, we fit to the transform of the Kohlrausch function

$$\varepsilon''(\omega) = \Delta\varepsilon\omega\int_0^\infty \varepsilon(t)\cos(\omega t)\,\mathrm{d}t \tag{3}$$

where

$$\varepsilon(t) = \exp[-(t/\tau_K)^\beta] \tag{4}$$

in which $\Delta\varepsilon$ is the dielectric relaxation strength, ω is the angular frequency, and the stretch exponent is $0 < \beta \leq 1$. The Kohlrausch relaxation time, τ_K, is related to the τ_α defined as the inverse of the frequency of the peak maximum by an empirical equation[33]

$$\tau_K = (0.175\beta^2 + 0.266\beta + 0.560)\tau_\alpha \tag{5}$$

The global motion of unentangled polymers is usually described by the Rouse model, which gives for the dielectric loss

$$\varepsilon(t) = \Delta\varepsilon\frac{2}{N(N-1)}\sum_{podd}^{N-1}\cot^2\left(\frac{p\pi}{2N}\right)\exp(-t/\tau_p) \tag{6}$$

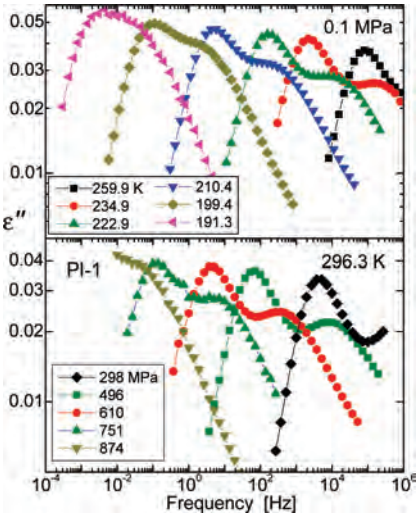

Figure 1. Dielectric loss spectra of the lowest M_w PI measured at 0.1 MPa and various temperatures (upper) and at 296.3 K and various pressures (lower). With decreasing frequency of the peak maxima, there is increasing overlap of the segmental and normal modes.

for a chain of N subunits, each having a relaxation time

$$\tau_p = \frac{\pi^2\tau_0}{4\sin^2(p\pi/2N)} \tag{7}$$

For large N, eq 6 reduces to

$$\varepsilon(t) = \Delta\varepsilon\frac{8}{\pi^2}\sum_{p\ \mathrm{odd}}^{N-1} p^{-2}\exp(-t/\tau_p) \tag{8}$$

Historically, it has been assumed that the friction factor relevant to global chain motions is the local segmental friction coefficient, so that the τ_0 in eq 7 can be identified with τ_α. However, this equivalence cannot be correct, given the different temperature and pressure dependences of the Rouse and local segmental modes,[4−7] and thus in practice, τ_0 serves as an adjustable parameter. Whereas the Rouse spectrum accurately describes relaxation spectra on the low-frequency side of the peak, eq 6 underestimates experimental loss peaks at high frequencies.[34] We have previously reported a corresponding phenomenon in mechanical measurements[35] and offered an explanation in terms of the contribution of polymer motions involving ca. 10 backbone bonds. Such chain segments are too short to exhibit Gaussian statistics and thus are not included in the Rouse description (although, without invoking the Gaussian approximation, general equations of motion can be derived that have the qualitative form of the Rouse model[36]). Whereas the motion of these intermediate "sub-Rouse" modes[4,37] involves more than the couple of conformers involved in the local segmental dynamics, the latter serves as the precursor; that is, the backbone bond rotations comprising structural relaxation permit motion to proceed beyond the locally relaxing segments themselves. Provided the sub-Rouse modes are not subsumed by an intense segmental process, the sub-Rouse motion can be detected in mechanical measurements and by dielectric spectroscopy on type-A polymers.

To account for the sub-Rouse contribution as well as any effect of polydispersity,[38] we replaced the exponential function in eq 6 with a stretched exponential. Although there is no theory guiding the choice of a relaxation function for the sub-Rouse process, the use of eq 4 follows from previous work[39] and is consistent with the broadening toward higher frequencies seen in molecular dynamics simulations.[40−43] A representative fit is shown in

Table 2. VFTH Parameters (eq 9) at Ambient Pressure

	PI-1		PI-10		PI-20	
	segmental	normal mode	segmental	normal mode	segmental	normal mode
$\log(\tau_\infty/s)$	−14.5	−12.4	−13.3	−9.2	−12.4	−8.1
D_T	12.85	15.38	8.37	9.87	7.12	10.04
T_0 [K]	140.0	130.6	165.6	157.0	170.2	157.1

Table 3. Isothermal VFTH Parameters (eq 10)

		segmental				normal mode			
PI-1	T [K]	230.1	249.4	274.3	296.3	230.1	249.4	274.3	296.3
	$\log(\tau_0/s)$	−5.94	−7.48	−8.60	−9.15	−3.74	−5.15	−6.26	−6.81
	D_P	35.0	35.0	35.0	35.0	54.7	54.7	54.7	54.7
	P_0 [MPa]	822.7	1224	1756	2313	1264	1824	2538	3273

		segmental		normal mode	
PI-20	T [K]	251.1	298.2	251.1	298.2
	$\log(\tau_0/s)$	−6.25	−9.10	−1.02	−3.19
	D_P		37.9		49.0
	P_0 [MPa]	828.0	1615	1019	2121

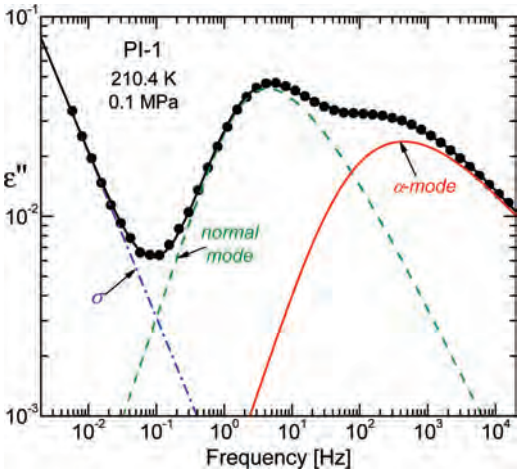

Figure 2. Dielectric loss showing the dc conductivity, normal mode, and local segmental relaxation. The spectra were fitted assuming independent contributions from the three processes.

Figure 2, which includes a power-law conductivity term ($\sigma \approx \omega^{-0.84\pm0.02}$) representing the contribution of mobile charge carriers. For the normal mode, the stretch exponent was a constant $\beta = 0.7 \pm 0.1$, whereas $\beta = 0.47$ for the local segmental relaxation at this T and P. Values determined at all temperatures and ambient pressure are displayed in Figure 3. The β increases somewhat (narrower dispersion) on cooling, contrary to the usual behavior.[44] This may be due to decreasing overlap of the secondary relaxation in PI.[45] Closer to T_g, this secondary relaxation is well-separated from the α-peak, and the shape of the latter becomes essentially constant.

Relaxation Times. The isobaric τ_α and τ_N for PI-1 were fit to the empirical Vogel−Fulcher−Tammann−Hesse (VFTH) equation[46]

$$\tau(T) = \tau_\infty \exp\left(\frac{D_T T_0}{T - T_0}\right) \quad (9)$$

in which T_0 and τ_∞ are temperature-independent, and D_T is assumed to be independent of T. The corresponding isothermal data were fit to the pressure-equivalent of the VFTH equation[47]

$$\tau(P) = \tau_0 \exp\left(\frac{D_P P}{P_0 - P}\right) \quad (10)$$

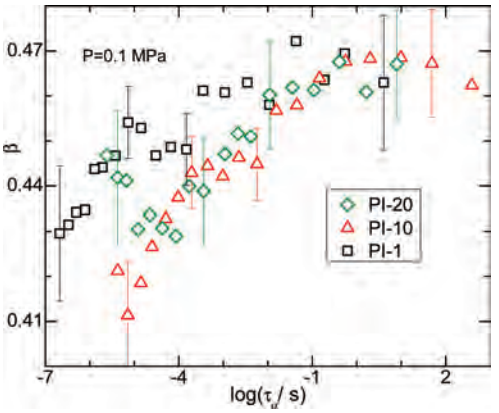

Figure 3. Kohlrausch exponent for α-relaxation peak for the polyisoprenes at ambient pressure.

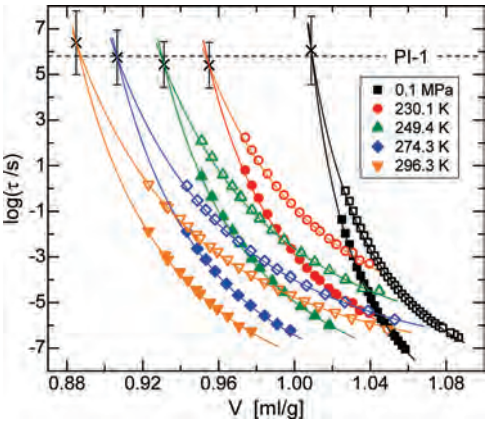

Figure 4. Local segmental (solid symbols) and normal mode (open symbols) relaxation times as a function of the specific volume. Changes in V were carried out by isobaric changes in T from 0 to −74 °C (squares) or isothermal changes in P up to as high as 750 MPa (all other symbols).

where P_0 is independent of pressure, D_P is pressure and temperature independent, and τ_0 is $\tau(T)$ from eq 9 at the temperature of the isotherm. Fit parameters are listed in Tables 2 and 3. The relaxation times are plotted in Figure 4 as a function of the specific volume, the latter calculated for each state point from the Tait equation of state (EoS)

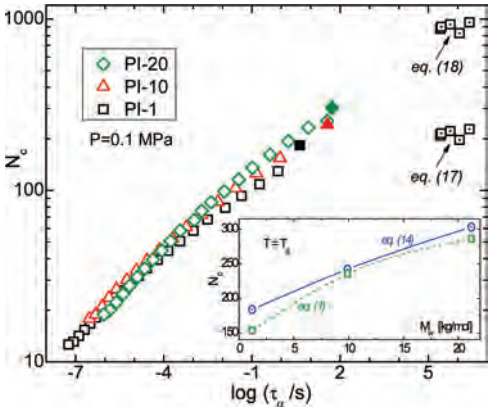

Figure 5. Number of dynamically correlated PI repeat units calculated at various temperatures from χ_T (eq 1; open symbols), measured at T_g by calorimetry ξ^3 (eq 14; solid symbols), and determined for PI-1 from the merging of the segmental and normal mode relaxation times (dotted squares; based on either eq 17 or 18, which assume different relations between length and volume). For N_c from τ_x, results for $P > 0.1$ MPa are included because the correlation volume depends only on τ_α. The inset shows the values of N_c at the calorimetric T_g from χ_T and DSC.

determined from the PVT measurements on PI-1

$$V(T,P) = 1.080(\exp[7.14\times10^{-4}T])\left[1-0.0894\ln\left(1+\frac{P}{168.91\exp[-4.96\times10^{-3}T]}\right)\right] \quad (11)$$

For PI-20, we used the EoS from the literature[5]

$$V(T,P) = (1.094+6.29\times10^{-4}T+6.23\times10^{-7}T^2)\left[1-0.0894\ln\left(1+\frac{P}{202\exp[-4.65\times10^{-3}T]}\right)\right] \quad (12)$$

In Figure 4, there is a barely significant increase with pressure in the (extrapolated) relaxation times at the intersection; the mean value $\tau_x = 6.5\ (\pm2.0)\times10^5$ s.

Dynamic Heterogeneity. If the dielectric loss has the Kohlrausch form with a stretch exponent that is essentially invariant to temperature, then eq 1 can be rewritten as[48]

$$N_c = \frac{k_B}{\Delta c_p}\frac{N_A}{m}\left(\frac{\beta}{e}\right)^2\left(\frac{\mathrm{d}\ln\tau_\alpha}{\mathrm{d}\ln T}\right)^2 \quad (13)$$

N_c values determined using eq 13 are plotted in Figure 5 versus τ_α for the three PI samples, with the values for $\tau_\alpha = 1$ s listed in Table 1. The measurements at higher pressures were obtained as isotherms, so application of eq 13 is subject to large error; however, it has been shown that N_c depends only on τ_α,[49,50] independently of T and P, so that the curves in Figure 5 apply to all pressures. Approaching T_g, the dynamic correlations grow, with N_c attaining values exceeding the DP of the polymer chain. At the highest temperatures in Figure 5, $N_c \approx 10$, although away from T_g eq 1 is less accurate.[50,51] Eventually, N_c would go to unity with loss of all intermolecular cooperativity, as Debye behavior ($\beta = 1$) and an Arrhenius T-dependence emerge.

There is a systematic increase in N_c with molecular weight, which can be ascribed to the increasing mobility (configurational entropy) conferred by the chains ends, thereby facilitating rearrangements and reducing the correlation volume. The chain-end concentration decreases from ~10 mol % to <0.5% over the range of molecular weights herein.

The Kohlrausch exponent, a measure of the degree of dispersity of the relaxation, is expected to be related to the dynamic heterogeneity reflected in N_c. This expectation is borne out in molecular dynamics simulations, wherein N_c can be calculated exactly for $\chi_4(t)$.[26,49] Comparing Figures 3 and 5, the increasing dynamic correlation volume is not accompanied by an increase in the dispersity of the relaxation function. In general, among different materials, there is an absence of any correlation between β and N_c.[26] Such behavior is consistent with the idea that the increase in the spatial extent of the dynamic correlations underlying the growth of the dynamic susceptibility need not be related to the magnitude of the local fluctuations. It is the latter that determines the variation in molecular relaxation times within the correlation volume and hence β.

On the basis of assumptions concerning the effect of enthalpy fluctuations on molecular motions similar to those underlying eq 1, Donth[27] derived an expression for the correlation volume

$$N_c(T) = \frac{N_A k_B T^2 \Delta c_p^{-1}}{m(\delta T^2)} \quad (14)$$

in which δT is the peak breadth of the imaginary component of the heat capacity, Δc_p^{-1} is the difference in the inverse of the isobaric heat capacities for the liquid and glass at T_g (note that the choice of Δc_p^{-1} rather than the $(\Delta c_p)^{-1}$ in eq 1 is arbitrary). The repeat unit volume v_m is calculated from the EoS (eq 11). These N_c values are plotted in Figure 5 for the value of the τ_α corresponding to the calorimetric T_g. The agreement between the two methods is satisfactory, as expected because eq 1 is most accurate near T_g.

Assuming that temperature and polarization fluctuations have approximately the same spectral shape, Saiter and coworkers[52] proposed a variation on eq 14, whereby δT is taken as the width of the dielectric loss peak in an isochronal $\varepsilon''(T)$ measurement. As shown in the Appendix, this approach yields eq 13 to within a numerical constant. Moreover, the method has the advantage over heat capacity spectroscopy of potentially enabling N_c to be determined over a much broader range of τ_α. However, it was not applied herein because of the difficulties of deconvoluting in the temperature domain the overlapping segmental and normal mode peaks.

The determinations of N_c described above consider only the local segmental dynamics; analysis of the normal mode is necessary only to deconvolute the two processes. Schönhals and Schlosser[28] proposed a method of estimating the dynamic correlation length based on the intersection of the two relaxations. The different T-dependences of τ_α and τ_N cause their merging at lower temperature, which is interpreted as corresponding to conditions under which the length scale of the two processes become equivalent.[28] Therefore, the correlation length for the segmental dynamics is obtained from the end-to-end chain length because the dielectric normal mode is due to fluctuations of the end-to-end vector;[2] that is

$$\xi(T) = \langle r^2\rangle^{1/2} \quad (15)$$

The mean square end-to-end distance of the chain, $\langle r^2\rangle$, for $M > 1.5$ kD is given by (in units of nanometers)[53]

$$\log\langle r^2\rangle = \log M - 2.14 \quad (16)$$

Although in principle $\langle r^2\rangle$ depends on thermodynamic conditions, the change over the range of T and P herein is <0.3% (as affirmed from the constant dielectric strength of the normal mode) and thus neglectable. From the value of

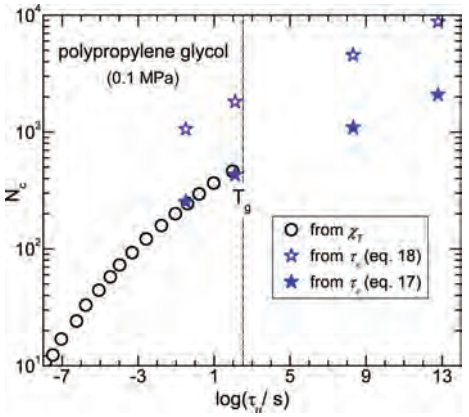

Figure 6. Number of dynamically correlated PPG repeat units determined from χ_T (open circles) at various temperatures and from τ_x (solid stars: eq 17; open stars: eq 18) at four temperatures (corresponding to the respective T_x for four molecular weights). Dielectric data are from ref 13.

τ_x, N_c can be obtained using[54]

$$N_c = \langle r^2 \rangle^{3/2} / v_m \tag{17}$$

or alternatively[27]

$$N_c = \frac{4}{3} \pi \langle r^2 \rangle^{3/2} / v_m \tag{18}$$

These equations, which assume a fairly compact shape, yield order of magnitude estimates; in reality, regions of correlation are probably fractal or string-like.[55,56]

The results for N_c from τ_x are displayed in Figure 5. We include the values of N_c for elevated pressure because $\langle r^2 \rangle$ is constant and N_c depends only on τ_α, independent of T and P.[49,50] Note that τ_x for PI-1 was obtained by extrapolation to the glassy state, in which dynamic fluctuations are arrested by the cessation of segmental motions at T_g; however, because the extrapolation assumes continuation of the liquid behavior, the obtained N_c represent the equilibrium values, as do the N_c from χ_T. Given the ill-defined shape of the correlation volume,[55,56] there is no discrepancy among the different determinations of N_c.

Gainaru et al.[13] carried out a similar analysis on PPG, determining N_c from the merging of τ_N and τ_α for four different molecular weight samples. Because PPG forms hydrogen bonds involving the terminal hydroxyl groups, the effect of chain ends is suppressed (as seen, for example, in the weak M-dependence of T_g for PPG[57]). Accordingly, Gainaru et al.[13] made the assumption that N_c is independent of M so that the change in N_c for these samples (i.e., the change in $T(\tau_x)$ with M) was interpreted as reflecting the temperature dependence of the correlation volume. These results are reproduced in Figure 6, along with our calculations of N_c using eq 1 and the dielectric data in ref 13. Consistent with the results for PI (Figure 5), the rate of growth of N_c slows with increasing τ_α.

Density Scaling. Previously, we used published data measured at pressures to 350 MPa and reported that the segmental and normal mode relaxation times of PI with M = 11 kg/mol superposed according to eq 2 with γ = 3.0 ± 0.25. The uncertainty of the analysis was substantial because the relaxation times above ambient pressure comprised only two isotherms spanning less than four decades of τ. As seen in Figure 4, the measurements herein include four isotherms (extending to pressures as high 750 MPa), with τ measured over six decades. These relaxation times are plotted versus

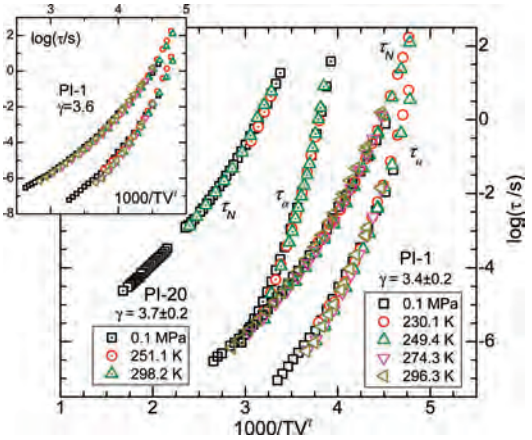

Figure 7. Density-scaled plots of the relaxation times for the lowest (open symbols) and highest M_w (dotted symbols). Each symbol is a distinct isotherm or isobar. The value of γ was chosen to minimize the least-squares deviation from superpositioning for both processes. The inset shows the data for PI-1 scaled using the γ (= 3.6) that maximizes overlap of the normal mode relaxation times.

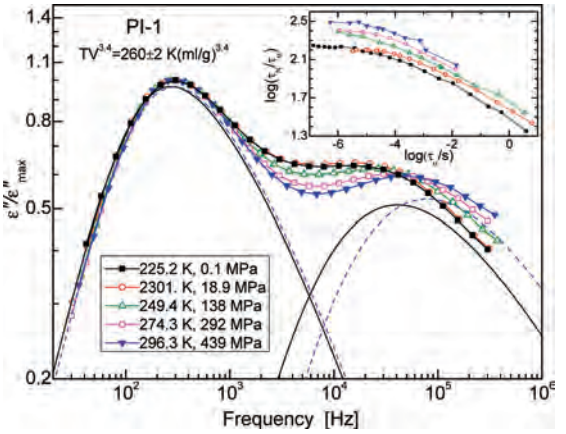

Figure 8. Dielectric loss spectra obtained under various conditions of T and P such that the frequency of the normal mode peaks coincide. (Vertical shifting was used to superpose the peak maxima.) The deconvoluted peaks are indicated for the spectra at the lowest (solid lines) and highest (dashed lines) pressures. The α-peaks do not superpose, revealing the breakdown of the scaling. The inset shows the increase in the separation of the two peaks as pressure increases; that is, at constant τ_α, there is a decrease in τ_N.

TV^γ in Figure 7. For PI-1, the superposed data overlap more than six decades, with some scatter in τ_α because of the need to deconvolute the normal mode peak. The scalings of τ_N and τ_α were carried out assuming a common value of γ. This assumption is acceptable within the uncertainty of the superpositioning procedure, and as shown in the inset to Figure 7, adjusting γ to optimize overlap of the τ_N has a negligible effect on the scaling. The reported γ minimizes the sum-of-squares of the difference between the data points, $\tau(TV^\gamma)$, and a global fit of a third degree polynomial to the superposed data.

A more direct test of whether the scaling exponent is the same for the terminal and segmental modes is by examination of the loss spectra. In Figure 8, the dielectric loss is shown for five state points for which the product variable $TV^{3.4}$ is constant (= 260 ± 2 in units of K and mL/g). The normal mode peak frequencies are the same; however, there is a systematic shift of the α-peak toward higher frequency with increasing pressure, indicating that the scaling relation for τ_N and τ_α cannot be the same assuming no interference from sub-Rouse modes. This difference in their respective γ causes a

change in the ratio τ_N/τ_α, as shown in the inset to Figure 8. This result agrees with recent data from Pawlus et al.[21] Note, however, that the stronger sensitivity to T and P of segmental relaxation compared to the global dynamics[4−7] is due to differences in the f in eq 2, rather than the exponent γ.

γ for the α-process is somewhat larger for the higher M PI, a different result than that found previously for PMMA[58] and PS.[59] To quantify the relative contribution of temperature and volume to the dynamics, we calculate the ratio of the isochoric, E_V, and isobaric, E_P, activation energies using the equation[31]

$$\frac{E_V}{E_P} = (1+\gamma T\alpha_P)^{-1} \tag{19}$$

The result is $E_V/E_P = 0.69 \pm 0.01$ at T_g. This value, consistent with recent results for a high-molecular-weight natural rubber,[60] is larger than 0.5, indicating that temperature is the stronger control variable for the segmental dynamics than is volume. This is generally the case for polymers,[31] notwithstanding the historical attraction of free volume models in describing their dynamic properties.[46]

Summary

The number of dynamically correlated chain segments has been determined for polyisoprenes of different molecular weights using three methods to obtain N_c. The results are reasonably consistent, although such comparisons are hindered by the uncertain connection between correlation lengths and correlation volumes. In the usual fashion, the number of correlating chain segments grows with increasing τ_α, attaining values that can exceed the degree of polymerization of the polymer. At given τ_α, N_c increases with increasing molecular weight because of the loss of the motional freedom conferred by the chain ends.

Both the local segmental and normal mode relaxation times superpose as a function of TV^γ. Whereas the scaling can ostensibly be achieved using the same value of the exponent for both modes, there actually is a small difference in the respective γ for τ_N and τ_α. This is consistent with their different T-, P-, and V-dependences near T_g.

Acknowledgment. This work was supported by the Office of Naval Research. D.F. and R.B. acknowledge postdoctoral fellowships from the National Research Council and the American Society for Engineering Education, respectively.

APPENDIX: Correlation Volume from $\varepsilon''(T)$

Assuming that the α-relaxation is described by eq 4, the width of a Gaussian fit to the peak in the frequency domain, $\delta \ln \omega$ ($= \delta \ln \tau_\alpha$) is given by $\delta \ln \tau \approx 1.07/\beta$.[61] Neglecting any variation of β within the temperature interval δT, this peak width can be approximated by

$$\delta T \approx \frac{\delta \ln \tau}{\partial \ln \tau/\partial T} = \frac{1.07T}{\beta}\left(\frac{\mathrm{d} \ln \tau_\alpha}{\mathrm{d} \ln T}\right)^{-1} \tag{A1}$$

Substituting into the fluctuation formula (eq 14) gives

$$N_c = 0.87 k_B \Delta(1/c_p)\beta^2 \frac{N_A}{m}\left(\frac{\mathrm{d} \ln \tau_\alpha}{\mathrm{d} \ln T}\right)^2 \tag{A2}$$

which differs from eq 13 by a numerical constant and the manner in which the heat capacity change is taken into account.

References and Notes

(1) Stockmayer, W. H. *Pure Appl. Chem.* **1967**, *15*, 539.
(2) *Broadband Dielectric Spectroscopy*; Kremer, F., Schonhals, A., Eds.; Springer-Verlag: New York, 2003.
(3) Watanabe, H. *Macromol. Rapid Commun.* **2001**, *22*, 127.
(4) Ngai, K. L.; Plazek, D. J. *Rubber Chem. Technol.* **1995**, *68*, 376.
(5) Floudas, G.; Reisinger, T. *J. Chem. Phys.* **1999**, *111*, 5201.
(6) Roland, C. M.; Psurek, T.; Pawlus, S.; Paluch, M. *J. Polym. Sci., Part B: Polym. Phys.* **2003**, *41*, 3047.
(7) Ngai, K. L.; Casalini, R.; Roland, C. M. *Macromolecules* **2005**, *38*, 4363.
(8) Mierzwa, M.; Floudas, G.; Dorgan, J.; Knauss, D.; Wegner, J. *J. Non-Cryst. Solids* **2002**, *307*, 296.
(9) Kyritsis, A.; Pissis, P.; Mai, S. M.; Booth, C. *Macromolecules* **2000**, *32*, 4581.
(10) Casalini, R.; Roland, C. M. *Macromolecules* **2005**, *38*, 1779.
(11) Roland, C. M.; Casalini, R.; Paluch, M. *J. Polym. Sci., Polym. Phys.* **2004**, *42*, 4313.
(12) Gainaru, C.; Bohmer, R. *Macromolecules* **2009**, *42*, 7616.
(13) Gainaru, C.; Hiller, W.; Bohmer, R. *Macromolecules* **2010**, *43*, 1907.
(14) Hirai, T.; Fujimura, N.; Urakawa, O.; Adachi, K.; Donkai, M.; Se, K. *Polymer* **2002**, *43*, 1133.
(15) Hirose, Y.; Adachi, K. *Polymer* **2005**, *46*, 1913.
(16) Roland, C. M.; Bero, C. A. *Macromolecules* **1996**, *29*, 7521.
(17) Schroeder, M. J.; Roland, C. M. *Macromolecules* **1999**, *32*, 2000.
(18) Imanishi, Y.; Adachi, K.; Kotaka, T. *J. Chem. Phys.* **1988**, *89*, 7585.
(19) Watanabe, H.; Urakawa, O.; Yamada, H.; Yao, M.-L. *Macromolecules* **1996**, *29*, 755.
(20) Boese, D.; Kremer, F.; Fetters, L. J. *Macromolecules* **1990**, *23*, 1826.
(21) Pawlus, S.; Sokolov, A. P.; Paluch, M.; Mierzwa, M. *Macromolecules* **2010**, *43*, 5845.
(22) Glotzer, S. C.; Novikov, V. N.; Schroder, T. B. *J. Chem. Phys.* **2000**, *112*, 509.
(23) Berthier, L.; Biroli, G.; Bouchaud, J.-P.; Cipelletti, L.; El Masri, D.; L'Hote, D.; Ladieu, F.; Pierno, M. *Science* **2005**, *310*, 1797.
(24) Chandler, D.; Garrahan, J. P.; Jack, R. L.; Maibaum, L.; Pan, A. C. *Phys. Rev. E* **2006**, *74*, 051501.
(25) Berthier, L.; Biroli, G.; Bouchaud, J.-P.; Kob, W.; Miyazaki, K.; Reichman, D. R. *J. Chem. Phys.* **2007**, *126*, 184503.
(26) Roland, C. M.; Fragiadakis, D.; Coslovich, D.; Capaccioli, S.; Ngai, K. L. *J. Chem. Phys.* **2010**, *133*, 124507.
(27) Donth, E. *J. Non-Cryst. Solids* **1982**, *53*, 325.
(28) Schönhals, A.; Schlosser, E. *Phys. Scr.* **1993**, *T49A*, 233.
(29) Hall, C. K.; Helfand, E. *J. Chem. Phys.* **1982**, *77*, 3275.
(30) Roland, C. M. *Macromolecules* **2010**, *43*, 7875.
(31) Roland, C. M.; Hensel-Bielowka, S.; Paluch, M.; Casalini, R. *Rep. Prog. Phys.* **2005**, *68*, 1405.
(32) Zoller, P.; Walsh, D. J. *Standard Pressure-Vol.-Temperature Data for Polymers*; Technomic: Lancaster, PA, 1995.
(33) Santangelo, P. G., unpublished.
(34) Adachi, K.; Kotaka, T. *Prog. Polym. Sci.* **1993**, *18*, 585.
(35) Plazek, D. J.; Chay, I.-C.; Ngai, K. L.; Roland, C. M. *Macromolecules* **1995**, *28*, 6432.
(36) Fatkullin, N. F.; Shakirov, T. M.; Balakirev, N. A. *Vysokomol. Soedin., Ser. A* **2010**, *52*, 72.
(37) Santangelo, P. G.; Ngai, K. L.; Roland, C. M. *Macromolecules* **1993**, *26*, 2682.
(38) Riedel, C.; Alegria, A.; Tordjeman, P.; Colmenero, J. *Macromolecules* **2009**, *42*, 8492.
(39) Abou Elfadl, A.; Kahlau, R.; Herrmann, A.; Novikov, V. N.; Rossler, E. A. *Macromolecules* **2010**, *43*, 3340.
(40) (a) Kreer, T.; Baschnagel, J.; Müller, M.; Binder, K. *Macromolecules* **2001**, *34*, 1105. (b) Binder, K.; Baschnagel, J.; Paul, W. *Prog. Polym. Sci.* **2003**, *28*, 115.
(41) Doxastakis, M.; Theodorou, D. N.; Fytas, G.; Kremer, F.; Faller, R.; Mueller-Plathe, F.; Hadjichristidis, N. *J. Chem. Phys.* **2003**, *119*, 6883.
(42) Smith, G. D.; Borodin, O. J.; Paul, W. *J. Chem. Phys.* **2002**, *117*, 10350.
(43) Padding, J. T.; Briels, W. J. *J. Chem. Phys.* **2002**, *117*, 925.
(44) Casalini, R.; Ngai, K. L.; Roland, C. M. *Phys. Rev. B* **2003**, *68*, 014201.
(45) Roland, C. M.; Schroeder, M. J.; Fontanella, J. J.; Ngai, K. L. *Macromolecules* **2004**, *37*, 2630.
(46) Ferry, J. D. *Viscoelastic Properties of Polymers*, 3rd ed.; Wiley: New York, 1980.
(47) Johari, G. P.; Whalley, E. *Faraday Symp. Chem. Soc.* **1972**, *6*, 23.
(48) Capaccioli, S.; Ruocco, G.; Zamponi, F. *J. Phys. Chem. B* **2008**, *112*, 10652.
(49) Coslovich, D.; Roland, C. M. *J. Chem. Phys.* **2009**, *131*, 151103.
(50) Fragiadakis, D.; Casalini, R.; Roland, C. M. *J. Phys. Chem. B* **2009**, *113*, 13134.

(51) Dalle-Ferrier, C.; Thibierge, C.; Alba-Simionesco, C.; Berthier, L.; Biroli, G.; Bouchaud, J. P.; Ladieu, F.; L'Hote, D.; Tarjus, G. *Phys. Rev. E* **2007**, *76*, 041510.
(52) Saiter, A.; Delbreilh, L.; Couderc, H.; Arabeche, K.; Schönhals, A.; Saiter, J.-M. *Phys. Rev. E* **2010**, *81*, 014805.
(53) Adachi, K.; Nishi, I.; Itoh, S.; Kotaka, T. *Macromolecules* **1990**, *23*, 2550.
(54) Hempel, E.; Hempel, H.; Hensel, A.; Schick, C.; Donth, E. *J. Phys. Chem. B* **2000**, *104*, 2460.
(55) Schroder, T. B.; Sastry, S.; Dyre, J. C.; Glotzer, S. C. *J. Chem. Phys.* **2000**, *112*, 9834.
(56) Stevenson, J. D.; Schmalian, J.; Wolynes, P. G. *Nat. Phys.* **2006**, *2*, 268.
(57) Engberg, D.; Schüller, J.; Strube, B.; Sokolov, A. P.; Torell, L. M. *Polymer* **1999**, *40*, 4755.
(58) Casalini, R.; Roland, C. M.; Capaccioli, S. *J. Chem. Phys.* **2007**, *126*, 184903.
(59) Roland, C. M.; McGrath, K. J.; Casalini, R. *J. Non-Cryst. Solids* **2006**, *352*, 4910.
(60) Ortiz-Serna, P.; Diaz-Calleja, R.; Sanchis, M. J.; Floudas, G.; Nunes, R. C.; Martins, A. F.; Visconte, L. L. *Macromolecules* **2010**, *43*, 5094.
(61) Donth, E. *The Glass Transition: Relaxation Dynamics in Liquids and Disordered Materials*; Springer: Berlin, 2001; Table 2.3.